

Interactions between cancer stem cells and their niche govern metastatic colonization

Ilaria Malanchi^{1*}, Albert Santamaria-Martinez^{1*}, Evelyn Susanto¹, Hong Peng^{1,2}, Hans-Anton Lehr³, Jean-Francois Delaloye⁴ & Joerg Huelsken¹

Metastatic growth in distant organs is the major cause of cancer mortality. The development of metastasis is a multistage process with several rate-limiting steps¹. Although dissemination of tumour cells seems to be an early and frequent event², the successful initiation of metastatic growth, a process termed 'metastatic colonization', is inefficient for many cancer types and is accomplished only by a minority of cancer cells that reach distant sites^{3,4}. Prevalent target sites are characteristic of many tumour entities⁵, suggesting that inadequate support by distant tissues contributes to the inefficiency of the metastatic process. Here we show that a small population of cancer stem cells is critical for metastatic colonization, that is, the initial expansion of cancer cells at the secondary site, and that stromal niche signals are crucial to this expansion process. We find that periostin (POSTN), a component of the extracellular matrix, is expressed by fibroblasts in the normal tissue and in the stroma of the primary tumour. Infiltrating tumour cells need to induce stromal POSTN expression in the secondary target organ (in this case lung) to initiate colonization. POSTN is required to allow cancer stem cell maintenance, and blocking its function prevents metastasis. POSTN recruits Wnt ligands and thereby increases Wnt signalling in cancer stem cells. We suggest that the education of stromal cells by infiltrating tumour cells is an important step in metastatic colonization and that preventing *de novo* niche formation may be a novel strategy for the treatment of metastatic disease.

We aimed to explore limiting factors that determine metastatic success using the MMTV-PyMT mouse breast cancer model, which spontaneously metastasizes to the lungs⁶. We reasoned that the recently identified cancer stem cells (CSCs), also called tumour-initiating cells, a subset of cancer cells that allow long-term tumour growth and are thought to be responsible for remissions^{7,8}, might also be relevant to the development of metastatic disease (Supplementary Fig. 1). We measured the relative size of the population of CSCs from primary MMTV-PyMT tumours and their pulmonary metastases using the previously established markers CD90 and CD24, which label a subset of the CD24⁺CD29^{hi} or CD24⁺CD49^{hi} population used earlier to isolate CSCs and normal mammary gland stem cells^{9–13} (Supplementary Fig. 2). This CSC subset accounts for $3 \pm 2.1\%$ (s.d.) of all tumour cells from both primary tumours and metastases (Fig. 1a). When CD90⁺CD24⁺ CSCs or CD90⁺CD24⁻-depleted non-CSCs are separately isolated from GFP⁺ tumours and directly introduced into mice through tail vein injection (GFP, green fluorescent protein), only the CSC population is able to produce lung metastases (Fig. 1b). Moreover, CD90⁺CD24⁺ cells isolated subsequently from pulmonary metastases are again the only tumour cell population that efficiently initiates secondary metastases (Fig. 1c). This is not due to differences in the extravasation capabilities of CSCs and non-CSCs (Supplementary Fig. 3).

In time course experiments, the relative size of the CSC population changes drastically during metastatic colonization. When injecting unfractionated tumour cells, the total number of tumour cells in the lung declines rapidly within the first 7 d after seeding¹⁴ (Fig. 1d and Supplementary Fig. 4). Notably, the relative amount of CSCs transiently increases within the first and second weeks to more than 20%. This is due to selective expansion of the stem cell population as a result of their proliferation rate increasing over sixfold relative to the primary tumour in this early phase of metastatic colonization (as measured by BrdU incorporation; Fig. 1e and Supplementary Fig. 5). By contrast, non-CSCs show reduced proliferation 7 d after injection and, notably, fail to generate CSCs (Fig. 1e and Supplementary Fig. 6). Consequently, only CSCs are able to form metastatic colonies, and non-CSCs remain as single cells (Fig. 1f). Together, this demonstrates that selective expansion of CSCs is responsible for the initiation of metastasis.

The number of injected CSCs evidently exceeds the number of metastatic nodules, indicating that additional factors restrict successful metastatic colonization. Stem cells are suspected to rely on signals from their stromal environment, such as localized growth factors that can affect stem cell maintenance and proliferation^{15–17}. We identified *Postn* as a stromal factor of normal stem cell niches and the metastatic niche (Supplementary Methods). *Postn* encodes for periostin, which becomes incorporated in the extracellular matrix¹⁸ and has a role in bone, tooth and heart development and function^{19–21}. Its expression is downregulated in the adult except in niches in direct contact with tissue-specific stem cells in mammary gland, bone, skin and intestine (Fig. 2a and Supplementary Figs 7 and 8). In tumours, POSTN is produced by stromal α SMA⁺VIM⁺ (α SMA also known as ACTA2) fibroblasts according to RNA *in situ* hybridization, immunostaining and quantitative PCR (Fig. 2b–h). Notably, POSTN expression is induced in the lung stroma by infiltrating cancer cells (Fig. 2d), but does not occur in the alveolar lung tissue of tumour-bearing but metastasis-free animals (Supplementary Fig. 8). Human breast cancer patients show induction of stromal POSTN expression in 75% of lymph node metastases (Fig. 2i, j and Supplementary Fig. 9). Whereas POSTN-deficient mice maintain normal mammary gland development (Supplementary Figs 10–12), MMTV-PyMT *Postn*^{-/-} breast cancers show a dramatic decrease in the number and size of pulmonary metastases, to less than 10% of controls, despite unaltered primary tumour size and morphology ($n = 37$, $P < 0.003$; Fig. 3a–d and Supplementary Figs 13–15). Metastasis formation from POSTN-deficient tumour cells is rescued in wild-type recipients (Supplementary Figs 16 and 17), where expression of POSTN is at the same level as in controls (Supplementary Fig. 18), indicating that stromal production of POSTN determines metastatic efficiency.

In searching for tumour-derived factors that can induce stromal POSTN, *in silico* promoter analysis predicted regulation mediated

¹Ecole Polytechnique Fédérale de Lausanne, Swiss Institute for Experimental Cancer Research and National Center of Competence in Research 'Molecular Oncology', 1015 Lausanne, Switzerland.

²Nanfeng Hospital, Department of Otorhinolaryngology, Head and Neck Surgery, Southern Medical University, Guangzhou 510515, China. ³University Institute of Pathology, CHUV, University of Lausanne, 1011 Lausanne, Switzerland. ⁴Department of Gynecology and Obstetrics, Centre Hospitalier Universitaire Vaudois, 1011 Lausanne, Switzerland.

*These authors contributed equally to this work.

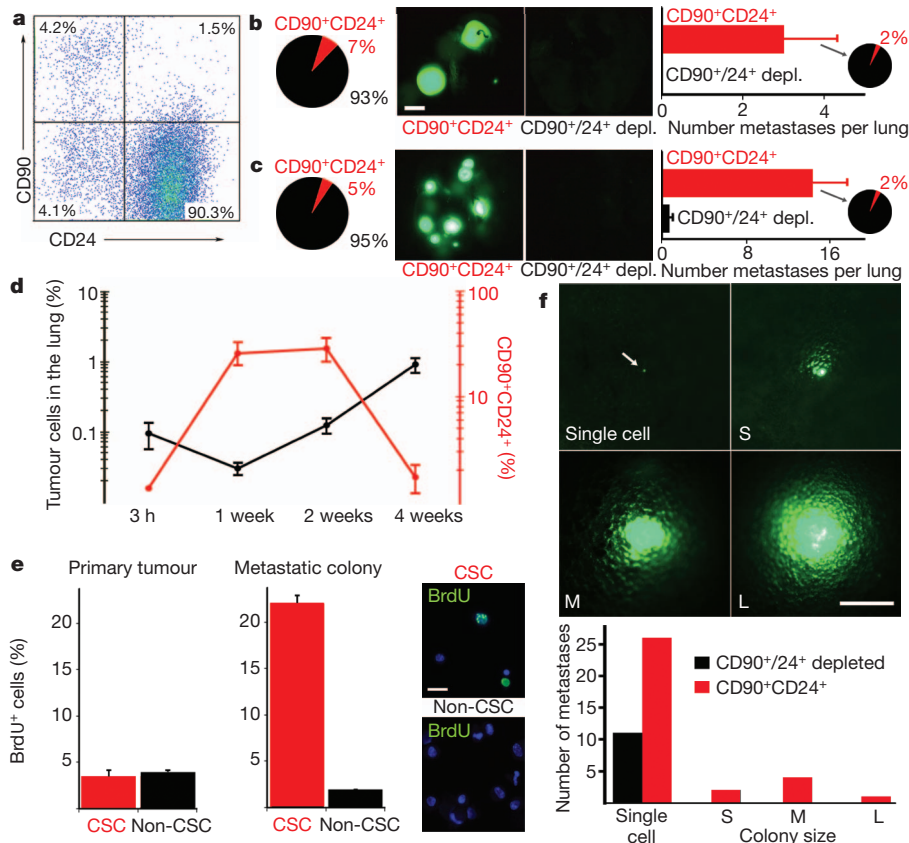


Figure 1 | Cancer stem cells initiate metastasis. (a) Representative density plot showing the abundance of cancer stem cells in MMTV-PyMT breast tumours defined as CD24⁺CD90⁺ after gating for viable (7-AAD⁻) and lin⁻ (CD31⁻CD45⁻TER119⁻) cells (not shown). **b, c**, CSCs are the only cells to form pulmonary metastases on tail vein injection. CD24⁺CD90⁺ CSCs and non-CSC populations from GFP⁺ tumour cells freshly isolated from primary tumours (**b**; 10⁴ cells injected each) and metastases (**c**; 10⁵ cells injected each) were separately injected in recipient mice. The frequency of CSCs (red; $P < 0.01$ (**b**), $P < 0.05$ (**c**)) is maintained at the metastatic site (shown as pie charts; $n = 6$ each; errors, s.e.m.). Scale bar, 1 mm. **d**, Time course experiments show selective proliferation of CSCs during metastatic colonization. GFP⁺ tumour cells (10⁶) were intravenously injected into recipient mice. At the indicated time points, the total proportion of GFP⁺ tumour cells in the lung (black line) and the relative amount of the CSC population (red line) were evaluated by analysis using fluorescence-activated cell sorting (FACS). Note the transient increase of

CSCs after one week ($n = 4$ per time point; errors, s.e.m.). **e, f**, CSCs are the only cells able to initiate growth in a short-term *in vivo* colonization assay. **e**, One week after tail vein injection of 10⁶ GFP⁺ tumour cells, mice were injected with BrdU. After 2 h, CSCs and non-CSCs were isolated by FACS and the frequency of proliferating cells was evaluated by BrdU staining on cytopins ($n = 12$, $P < 0.05$; errors, s.d.; representative example is shown on the right). Note the increase of proliferation in the CSC population during the early phase of lung colonization; by contrast, proliferation does not significantly differ between the two populations in the primary tumour. **f**, GFP⁺ CSCs (2 × 10⁵) or GFP⁺ non-CSCs (4 × 10⁵) were tail vein injected and analysed after two weeks. CD90⁺/CD24⁻-depleted non-CSCs remained as single cells whereas CSCs were able to initiate growth and form metastases of different sizes (S, 30–300 cells; M, 300–3,000 cells; L, >3,000 cells). The upper panel shows a representative example of the different metastasis colonies and the results are cumulatively quantified in the bottom panel ($n = 6$). Scale bars, 20 μm (**e**) and 250 μm (**f**).

by SMAD, NF-κB and LEF/TCF. Primary lung fibroblasts upregulate POSTN in response to TGF-β3 and TGF-β2, but are not responsive to BMP4, Wnt3A, Wnt5A or TNF-α (Fig. 3e, Supplementary Fig. 19 and data not shown). Co-culture experiments revealed that tumour cells are sufficient to trigger POSTN production (Supplementary Fig. 20). Notably, CSCs and non-CSCs both produce high levels of TGF-β3 (Supplementary Fig. 21), and blocking the action of TGF-β3 by expression of a secreted decoy receptor²² (TGFβR2ΔTM; see Methods) in tumour cells blocks POSTN expression and prevents metastasis formation (Fig. 3f and Supplementary Fig. 22) in line with earlier results²³. Together, these experiments demonstrate that infiltrating tumour cells need to educate the host stroma of the target organ to support metastasis initiation.

Even small metastatic colonies are strongly diminished in POSTN-deficient animals (Supplementary Fig. 23). Having shown that metastatic colonization depends on cancer stem cells, we went on to assess a potential role of POSTN in stem cell maintenance. Growth under conditions of ultralow attachment has been used to study CSCs *in vitro*²⁴. Surprisingly, establishment of such cancer stem cell cultures

is not possible using POSTN-deficient tumours (Fig. 3g–j; $n = 16$; compare with Supplementary Fig. 24, which shows unaltered cell survival in standard two-dimensional culture). In wild-type tumour spheres, POSTN is expressed by tumour-derived, stromal fibroblasts (Supplementary Fig. 25). Adding periostin protein to the mutant tumour cells rescues sphere formation (Fig. 3j). Conversely, a blocking antibody targeting POSTN prevents maintenance of wild-type cancer stem cells (Supplementary Fig. 30), but affects neither cellular survival nor growth *per se* (Supplementary Figs 26 and 27). Furthermore, CSCs fail to proliferate when co-cultured with POSTN-mutant, pulmonary fibroblasts (Fig. 3k). In lung metastases, we observe a preferential localization of CD90⁺ CSCs adjacent to stromal niches (Fig. 3l), whereas lung metastases in POSTN-deficient animals show a reduction in the size of the CSC population (Fig. 3m). Thus, POSTN is an essential niche factor that supports CSC growth during metastatic colonization.

To gain insight into how POSTN is related to the mechanisms that control stem cell maintenance, we characterized the interactome of POSTN by tandem affinity purification (TAP)-tag enrichment and

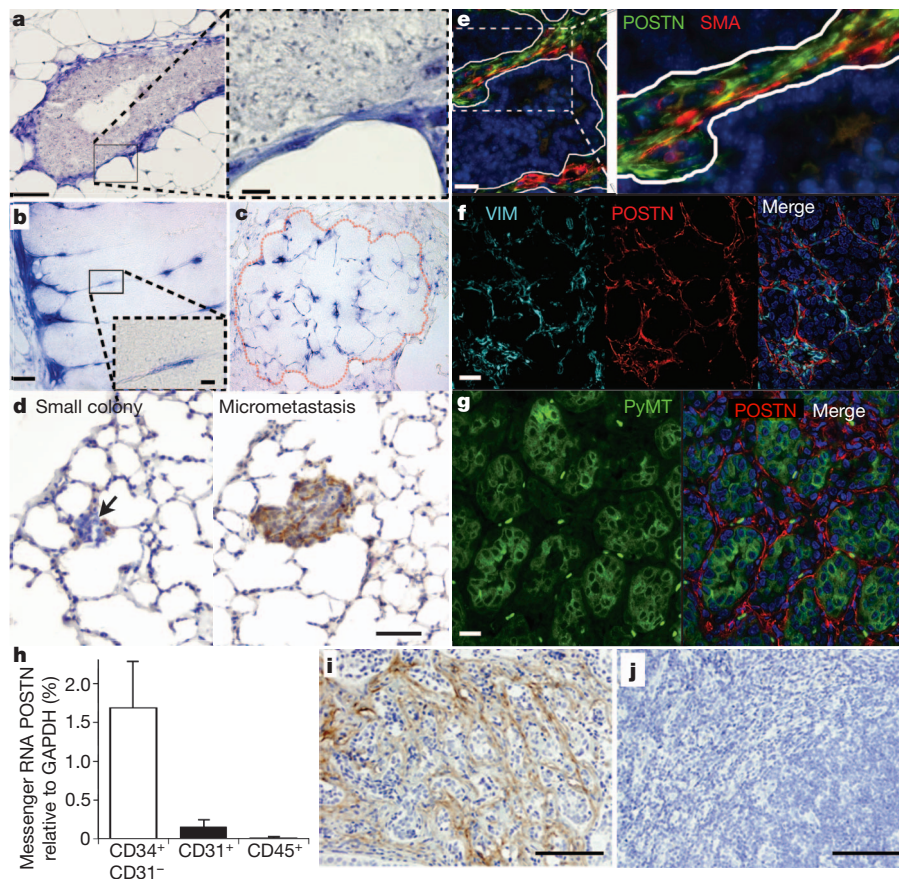


Figure 2 **POSTN is a stromal niche component that is induced on metastasis formation.** **a–c**, Stromal **POSTN** expression as detected by RNA *in situ* hybridization (**POSTN**-expressing cells in blue) around terminal end buds, which are enriched for mammary gland stem cells during puberty (**a**), tumour cells at the primary site (**b**) and in pulmonary metastases (**c**; outlined in red). **d**, Immunohistochemistry of **POSTN** expression in pulmonary metastases at different stages. **e–g**, Immunofluorescence analysis of **POSTN** and fibroblast markers in pulmonary metastases. **POSTN** is not expressed by PyMT tumour cells (**g**), but is from α SMA⁺ (**e**) and VIM⁺ (**f**) fibroblasts. The white outline in

e defines the tumour–stroma border. **h**, Quantitative PCR with reverse transcription detects **POSTN** expression in CD34⁺CD31[−] pulmonary fibroblasts, in CD31⁺ endothelial cells but not in CD45⁺ immune cells that were isolated by FACS from lungs of mice with macrometastases ($n = 3$; errors, s.d.). **i, j**, Immunohistochemistry of **POSTN** expression in auxiliary lymph nodes of human breast cancer patients with metastasis-free N0 disease (**j**) or metastatic disease (**i**). A total of 17 of 23 lymph node metastases were positive for **POSTN** expression. Scale bars: 20 μ m (**a**) and 2.5 μ m (**a**, inset); 50 μ m (**b**; same scale in **c**) and 10 μ m (**b**, inset); 50 μ m (**d**); 20 μ m (**e–g**); 200 μ m (**i, j**).

tandem mass spectrometry (Supplementary Methods), and this pointed to binding of **POSTN** to Wnt ligands²⁵. Using TAP-tag pull-downs, we confirmed interaction between **POSTN** and Wnt1 and Wnt3A, but found that a known inhibitory ligand of the pathway, DKK1, does not associate with **POSTN** (Fig. 4a, b and Supplementary Fig. 28). The interaction between **POSTN** and Wnt ligands boosts Wnt signalling activity as measured by LRP6 phosphorylation and reporter assays using Wnt1, Wnt2 and Wnt6 (Fig. 4c, d). The Wnt pathway is known to control stem cell maintenance in a variety of tissues, including mammary gland²⁶ and tumours^{8,27,28}. Indeed, addition of Wnt3A can rescue *in vitro* stem cell expansion in the absence of **POSTN** (Supplementary Figs 30 and 31). Furthermore, we find Wnt signalling activity to be concentrated in the CSC population *in vivo* as analysed by FACS (Fig. 4e, f). Here, we use a lentiviral reporter that allows Wnt-inducible GFP expression and constitutive labelling of individual reporter-containing cells by human CD2 (Supplementary Fig. 29). Wnt signalling activity in metastases is abrogated in the absence of **POSTN** (Fig. 4g; see Supplementary Fig. 29 for Wnt activity in tumour spheres). Similarly, we detect higher levels of the general Wnt target gene *Axin2* in metastases in wild-type hosts than in mutant hosts (Fig. 4h, i). Remarkably, metastasis of Wnt-driven breast cancer proves to be independent of stromal **POSTN** (Fig. 4j). Thus, **POSTN** acts as a niche component that can promote stem cell maintenance and metastatic colonization by augmenting Wnt signalling (Supplementary Fig. 1).

Thus, instrumental factors that contribute to the inefficiency of the metastatic process are the low abundance of CSCs, which are required to initiate growth at the secondary site, and incompatibilities with ‘foreign’ niches, which necessitate education of the target organ to resemble the primary microenvironment. Periostin is an essential component of this CSC-supportive niche and needs to be induced in the lung stroma by infiltrating tumour cells. Together with a recent report that implicated tumour-cell-derived tenascin C in breast cancer metastasis, these examples demonstrate an essential role for single proteins of the extracellular matrix in metastatic colonization^{29,30}.

Surprisingly, **POSTN** deficiency affects neither normal mammary gland development nor tumour formation or the relative size of the CSC population at the primary site (Supplementary Fig. 32). This may be due to a greater complexity and redundancy in the primary niche, such that the loss of a single factor can be tolerated. By contrast, loss of only one important factor, such as **POSTN**, prevents metastatic colonization in the presumably less supportive and less complex secondary site. Accordingly, the early phase of metastasis can be anticipated to be particularly sensitive to therapeutic intervention because the dependence of cancer cells on niche signals is probably highest in that phase. Targeting this metastatic niche promises to be less sensitive to rapid genetic changes in cancer cells and may not only prevent metastatic colonization but may also interfere with the survival of disseminated, dormant cancer cells.

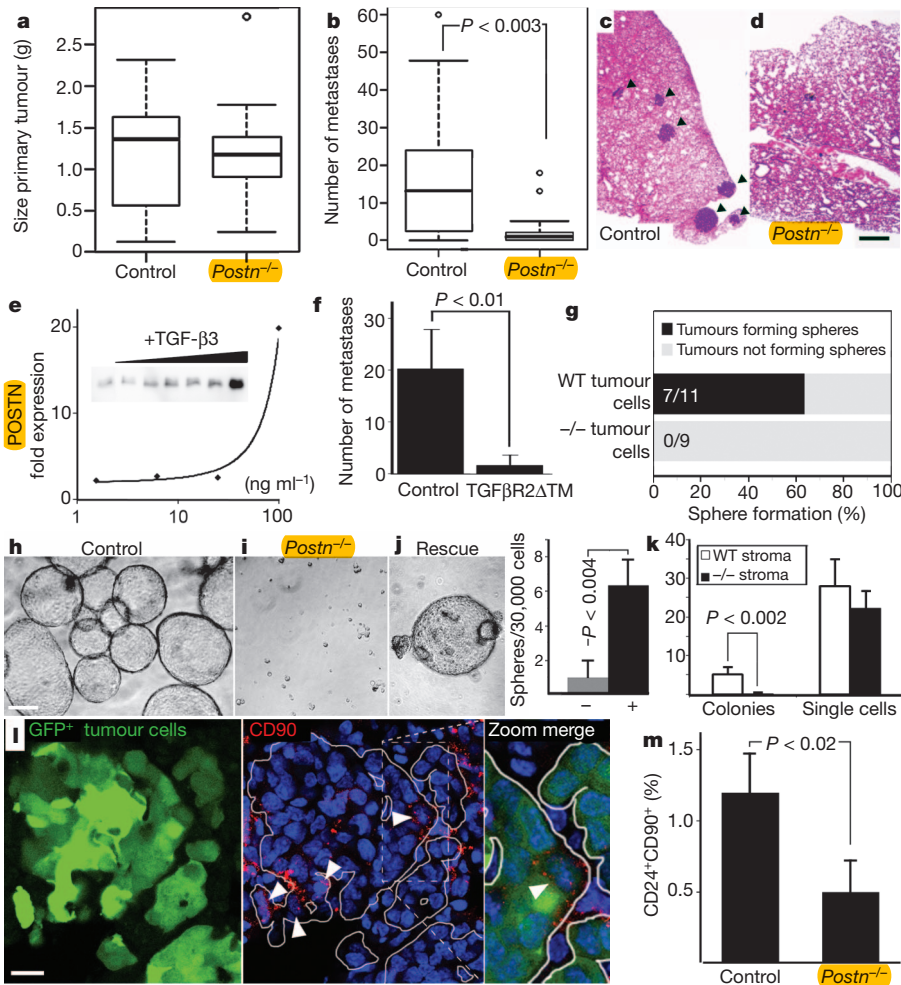


Figure 3 **POSTN** is required for metastatic colonization by affecting CSC maintenance. **a, b**, Primary tumour size (**a**) and number of spontaneously formed macrometastases (**b**) in control and *Postn*^{-/-} mice ($n = 37$). **c, d**, HE section of spontaneous, pulmonary metastases in control (**c**) and *POSTN*-mutant (**d**) animals. **e–f**, TGF- β 3 induces *POSTN* expression in lung stromal cells. **e**, TGF- β 3 was added to lung stromal cells to test its ability to induce *POSTN* expression. RNA expression by quantitative PCR and protein expression by western blot analysis (inset) were measured at the indicated concentrations. **f**, Blocking of TGF- β 3 abrogates metastasis formation. Cancer cells were infected either with a control virus or with a virus expressing secreted, dominant negative TGF β 2 Δ TM and separately intravenously injected into recipient mice. Metastasis formation was evaluated 6 weeks after injection ($n = 12$; errors, s.d.). **g**, Frequency of mammosphere formation from primary tumours. WT, wild type. **h**, Representative picture of control tumour mammospheres. **i**, Loss of CSCs in secondary mammosphere assays from *Postn*^{-/-} tumours. **j**, Sphere formation by *Postn*^{-/-} tumour cells can be rescued by addition of 50 ng ml⁻¹ of postistin to primary cultures. Control tumour cells produce 13.3 ± 2.5 spheres per 30,000 cells. Quantification is shown in the histogram on the right ($n = 4$; errors, s.d.). **k**, Only stromal cells isolated from wild-type lungs are able to support CSC colony formation *in vitro*. CSCs were sorted by FACS and seeded on lung stromal cells isolated either from wild-type or *Postn*^{-/-} mice. Colony formation was evaluated after two weeks ($n = 3$; errors, s.d.). **l**, Immunofluorescence analysis shows that GFP⁺CD90⁺ CSCs (white arrow heads) are concentrated in areas with immediate contact to the stroma. **m**, Reduced frequency of CD24⁺CD90⁺ CSCs in rare pulmonary metastases in *POSTN*-deficient mice ($n = 12$; errors, s.d.). Scale bars: 500 μ m (**c, d**); 50 μ m (**h–j**); 5 μ m (**l**).

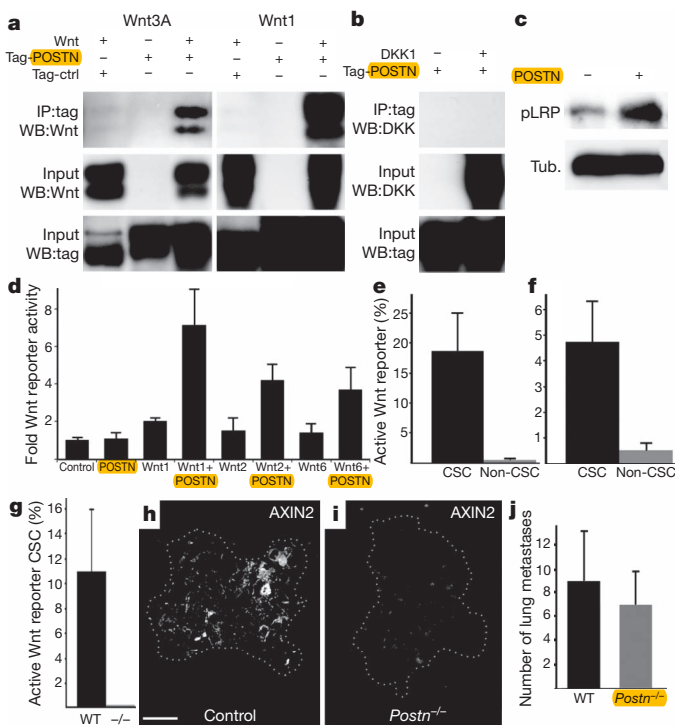


Figure 4 **POSTN** promotes stem cell maintenance and metastasis formation by augmenting Wnt signalling. **a**, Interaction of TAP-tagged *POSTN* and Wnt3A and Wnt1 as determined by pull down and western blotting. **b**, Interaction of TAP-tagged *POSTN* and DKK1 as determined by pull down and western blotting. Note the absence of interaction between *POSTN* and DKK1. **c**, LRP6 phosphorylation (pLRP) increases on *POSTN* expression. **d**, Wnt reporter activity in response to Wnt1, Wnt2 or Wnt6 is stimulated by *POSTN* ($n = 3$; errors, s.d.). **e, f**, *In vivo* Wnt reporter assay. Tumour cells were infected with a lentivirus containing both an artificial Wnt-responsive promoter driving GFP expression and a constitutive promoter expressing human CD2 (Supplementary Fig. 29). Cells were analysed by FACS considering only human-CD2⁺, reporter-containing cells. CD90⁺CD24⁺ CSCs and non-CSCs were scored for Wnt reporter activity as GFP⁺. The signal concentrates in CSCs in both primary tumours (**e**) and pulmonary metastases (**f**) ($n = 3$; errors, s.e.m.). **g**, CD90⁺CD24⁺ wild-type CSCs containing a Wnt reporter (human CD2⁺) show signalling activity (GFP⁺) only when seeded in wild-type as opposed to *Postn*^{-/-} lungs ($n = 3$; errors, s.e.m.). **h, i**, Immunofluorescence staining of AXIN2 in control (**h**) and *POSTN*-deficient (**i**) lung metastases (outlined in white). Note the absence of staining in *POSTN*^{-/-} lung metastases. Scale bar, 10 μ m. **j**, MMTV-Wnt1 tumour cells can form pulmonary metastases in the absence of *POSTN* expression in the stroma. Tumour cells were orthotopically transplanted into mammary glands of wild-type or *POSTN*-deficient recipients and analysed after ten weeks for spontaneous lung metastasis ($n = 5$ each; errors, s.d.).

METHODS SUMMARY

Details on the mouse models used and the generation of the *Postm* gene ablation can be found in Supplementary Information. Tumours derived from MMTV-PyMT mice were collected and cells were isolated and directly stained for FACS analysis or sorting using antibodies against CD31, CD45, TER119 (LY76), CD90, CD24 and CD49f (ITGA6). FACS-isolated tumour cells were directly transplanted into recipient mice.

Full Methods and any associated references are available in the online version of the paper at www.nature.com/nature.

Received 26 July 2010; accepted 1 November 2011.

Published online 7 December 2011.

- Chambers, A. F., Groom, A. C. & MacDonald, I. C. Dissemination and growth of cancer cells in metastatic sites. *Nature Rev. Cancer* **2**, 563–572 (2002).
- Hüsemann, Y. *et al.* Systemic spread is an early step in breast cancer. *Cancer Cell* **13**, 58–68 (2008).
- Kouros-Mehr, H. *et al.* GATA-3 links tumor differentiation and dissemination in a luminal breast cancer model. *Cancer Cell* **13**, 141–152 (2008).
- Nguyen, D. X., Bos, P. D. & Massague, J. Metastasis: from dissemination to organ-specific colonization. *Nature Rev. Cancer* **9**, 274–284 (2009).
- Hess, K. R. *et al.* Metastatic patterns in adenocarcinoma. *Cancer* **106**, 1624–1633 (2006).
- Lin, E. Y. *et al.* Progression to malignancy in the polyoma middle T oncoprotein mouse breast cancer model provides a reliable model for human diseases. *Am. J. Pathol.* **163**, 2113–2126 (2003).
- Al-Hajj, M., Wicha, M. S., Benito-Hernandez, A., Morrison, S. J. & Clarke, M. F. Prospective identification of tumorigenic breast cancer cells. *Proc. Natl Acad. Sci. USA* **100**, 3983–3988 (2003).
- Reya, T. & Clevers, H. Wnt signalling in stem cells and cancer. *Nature* **434**, 843–850 (2005).
- Cho, R. W. *et al.* Isolation and molecular characterization of cancer stem cells in MMTV-Wnt-1 murine breast tumors. *Stem Cells* **26**, 364–371 (2008).
- Shackleton, M. *et al.* Generation of a functional mammary gland from a single stem cell. *Nature* **439**, 84–88 (2006).
- Stingl, J. *et al.* Purification and unique properties of mammary epithelial stem cells. *Nature* **439**, 993–997 (2006).
- Liu, J. C., Deng, T., Lehal, R. S., Kim, J. & Zacksenhaus, E. Identification of tumorsphere- and tumor-initiating cells in HER2/Neu-induced mammary tumors. *Cancer Res.* **67**, 8671–8681 (2007).
- Zhang, M. *et al.* Identification of tumor-initiating cells in a p53-null mouse model of breast cancer. *Cancer Res.* **68**, 4674–4682 (2008).
- Podsypanina, K. *et al.* Seeding and propagation of untransformed mouse mammary cells in the lung. *Science* **321**, 1841–1844 (2008).
- Vermeulen, L. *et al.* Wnt activity defines colon cancer stem cells and is regulated by the microenvironment. *Nature Cell Biol.* **12**, 468–476 (2010).
- Visvader, J. E. & Lindeman, G. J. Cancer stem cells in solid tumours: accumulating evidence and unresolved questions. *Nature Rev. Cancer* **8**, 755–768 (2008).
- Psaila, B. & Lyden, D. The metastatic niche: adapting the foreign soil. *Nature Rev. Cancer* **9**, 285–293 (2009).
- Takehita, S., Kikuno, R., Tezuka, K. & Amann, E. Osteoblast-specific factor 2: cloning of a putative bone adhesion protein with homology with the insect protein fasciclin I. *Biochem. J.* **294**, 271–278 (1993).
- Shimazaki, M. & Kudo, A. Impaired capsule formation of tumors in periostin-null mice. *Biochem. Biophys. Res. Commun.* **367**, 736–742 (2008).
- Oka, T. *et al.* Genetic manipulation of periostin expression reveals a role in cardiac hypertrophy and ventricular remodeling. *Circ. Res.* **101**, 313–321 (2007).
- Rios, H. *et al.* Periostin null mice exhibit dwarfism, incisor enamel defects, and an early-onset periodontal disease-like phenotype. *Mol. Cell. Biol.* **25**, 11131–11144 (2005).
- Zhao, W. *et al.* Suppression of *in vivo* tumorigenicity of rat hepatoma cell line KDH-8 cells by soluble TGF-beta receptor type II. *Cancer Immunol. Immunother.* **51**, 381–388 (2002).
- Muraoka, R. S. *et al.* Blockade of TGF-beta inhibits mammary tumor cell viability, migration, and metastases. *J. Clin. Invest.* **109**, 1551–1559 (2002).
- Pece, S. *et al.* Biological and molecular heterogeneity of breast cancers correlates with their cancer stem cell content. *Cell* **140**, 62–73 (2010).
- Milovanovic, T. *et al.* Expression of Wnt genes and frizzled 1 and 2 receptors in normal breast epithelium and infiltrating breast carcinoma. *Int. J. Oncol.* **25**, 1337–1342 (2004).
- Zeng, Y. A. & Nusse, R. Wnt proteins are self-renewal factors for mammary stem cells and promote their long-term expansion in culture. *Cell Stem Cell* **6**, 568–577 (2010).
- Malanchi, I. *et al.* Cutaneous cancer stem cell maintenance is dependent on β -catenin signaling. *Nature* **452**, 650–653 (2008).
- Barker, N. *et al.* Crypt stem cells as the cells-of-origin of intestinal cancer. *Nature* **457**, 608–611 (2009).
- Wels, J., Kaplan, R. N., Rafii, S. & Lyden, D. Migratory neighbors and distant invaders: tumor-associated niche cells. *Genes Dev.* **22**, 559–574 (2008).
- Oskarsson, T. *et al.* Breast cancer cells produce tenascin C as a metastatic niche component to colonize the lungs. *Nature Med.* **17**, 867–874 (2011).

Supplementary Information is linked to the online version of the paper at www.nature.com/nature.

Acknowledgements We are grateful to U. Koch for advice on FACS, to M. Moniatte for advice on mass spectrometry and to S. Leuba for technical assistance with histology. I.M., E.S., A.S.-M. and J.H. were supported in part by the Swiss League against Cancer, the SNF, the NCCR in Molecular Oncology and the Anna Fuller Fund. J.H. holds the EPFL chair for Signal Transduction in Oncogenesis sponsored by Debiopharm.

Author Contributions I.M., A.S.-M. and J.H. designed and performed most of the experiments, analysed data and prepared the manuscript; E.S. and H.P. performed experiments; H.-A.L. performed experiments and analysed data; J.-F.D. provided clinical samples; and J.H. designed and supervised the study.

Author Information Reprints and permissions information is available at www.nature.com/reprints. The authors declare no competing financial interests. Readers are welcome to comment on the online version of this article at www.nature.com/nature. Correspondence and requests for materials should be addressed to J.H. (joerg.huelsken@epfl.ch).

METHODS

Mouse work. The design of the **POSTN** targeting vector is shown in Supplementary Fig. 10. E14.1 129/Ola ES cells were used for targeting and were injected into C57Bl6 blastocysts. The **POSTN** mutant allele was then backcrossed onto the FVB background for at least eight generations. The MMTV-PyMT³¹, MMTV-Wnt1³² and the ACT-GFP³³ mouse strains have been described previously. All used strains were backcrossed onto FVB for ten generations except for the Nude allele, which was used on a NMRI background. For tumour cell transplantations, *Nude* or *Rag1*^{-/-} mice were used when tumour cells expressed GFP or had been modified by lentiviral vectors. In general, we did not observe major differences in these different strains with respect to cancer stem cell phenotype, tumour take rate or metastasis number, except for an overall faster growth in *Rag1*^{-/-} versus *Nude* versus wild type. For tail vein injections, tumour cells were resuspended in 100 µl of PBS. For orthotopic transplantations, tumour cells were resuspended in 50 µl growth-factor-reduced matrigel (BD Biosciences) and transplanted into a small pocket within the fourth mammary fat pad. All animal procedures were performed in accordance with the Swiss legislation on animal experimentation.

Antibodies. We used TER119, CD24, CD29, CD34, CD45 and CD90.1 (eBioscience); CD31 and GFP (Invitrogen); Cytokeratin 8, **POSTN**, AXIN2 and Wnt1 (Abcam); **POSTN** (Adipogen); Cytokeratin 14 (Covance); GATA-3 and PyMT (Santa Cruz Biotechnology); αSMA (Sigma); VIM (Lifespan Biosciences); and BrdU (BD Pharmingen and ImmunologicalsDirect). The antibody against human CD2 was a kind gift by Professor Werner Held (Ludwig Center for Cancer Research, Lausanne).

Tumour and metastasis evaluation. For the quantification of spontaneous micrometastasis, lungs were completely sectioned and HE stained, and the size and the number of metastatic nodules were analysed by microscopy. Quantification of lung metastases derived from GFP⁺ tumour cells was performed by fluorescent microscopy (Leica M205 FA stereomicroscope) or by FACS analysis of cell preparations from total lungs. All statistical evaluation used a homoscedastic Student's *t*-test with a two-tailed distribution.

For expression of a secreted TGFβ decoy receptor (TGFβR2ΔTM), tumour cells were transduced with lentiviral vectors expressing the extracellular domain (amino acids 1–185) of murine TGFβR2 (NM_009371.3) under the control of a murine phosphoglycerate kinase (PGK) promoter, and metastases were scored as described above following tail vein injection of transduced tumour cells.

Tumour cell isolation. Tumours or lungs containing pulmonary metastases were minced with a razor blade and digested with a mixture of DNase and Liberase (Roche Diagnostics). On enzymatic digestion, samples were passed through a 100-µm filter and washed once in growth medium (DMEM/F12 with 2% FBS, 20 ng ml⁻¹ EGF, 10 µg ml⁻¹ insulin; Invitrogen) and twice in PBS. Cells were then directly used for FACS staining and analysed in a Cyan ADP flow cytometer (Beckman Coulter) or sorted with a custom-built FACS Aria II (Beckton Dickinson). For tail vein injection, cells were plated overnight on collagen. In the experiments evaluating the metastasis initiation potential of CSCs versus non-CSCs, we were able to prepare and inject higher cell numbers from metastases than from primary tumours, where larger necrotic areas limit the obtainable cell amounts. In both settings, only CSCs were able to give rise to pulmonary metastases, but this experimental setting is unsuitable for a direct comparison of the metastatic potential of CSCs isolated from primary tumours with that of those isolated from metastases. In the extravasation experiments, we performed several pilot experiments perfusing the lungs before dissection to distinguish cells trapped inside capillaries from those that successfully extravasated. Perfusion was done with Ringer's buffer through the right ventricle for 5–10 min.

Tumour mammosphere cultures. Sphere cultures were established from total tumour cell preparations. After dissociation, tumour cells were plated on collagen overnight, trypsinized and plated in 100 µl of sphere media (DMEM/F12 with B27, 20 ng ml⁻¹ EGF, 20 ng ml⁻¹ FGF and 4 µg ml⁻¹ heparin) into 96-well, low-attachment plates (Corning) at a concentration of (1–3) × 10⁴ cells per well. For the anti-**POSTN** blocking antibody assay, half of the culture medium was replaced by hybridoma supernatant. Secondary mammosphere culture was performed by collecting the spheres through gentle centrifugation (130g) followed by enzymatic (10 min in 0.05% trypsin-EDTA at 37 °C) and mechanical dissociation using a 25G needle. Immunostainings were performed as whole mounts of PFA-fixed and 0.1% Triton-X100-permeabilized spheres and were analysed by confocal microscopy.

Identification of POSTN as a niche-expressed factor. To identify niche-expressed factors, we performed microarray RNA profiling studies where we analysed laser-capture microdissected material from normal stem cells together with their adjacent stroma. This was compared with laser-capture microdissected material isolated from differentiated cells together with their adjacent stroma from the same tissue (data not shown). Skin and intestine contain stem cells in morphologically distinct structures (the bulge in the skin, the crypt in the intestine). On

the basis of these profiles (accessible through GEO GSE31730 and 8818), we evaluated potential niche localization of candidate genes by RNA *in situ* hybridization and immunofluorescence analysis (Fig. 2a, Supplementary Fig. 7 and data not shown). Moreover, we profiled the candidate genes by quantitative PCR with reverse transcription and performed RNA *in situ* hybridization in other tissues, in tumours and in metastases (data not shown). **This identified POSTN as a stromal marker in primary murine breast cancer and its metastases (Fig. 2).**

Immunodetection and in situ hybridization. Immunostaining was performed on 7-µm OCT- or gelatin-embedded (to maintain GFP signals) frozen sections permeabilized with 0.1% Triton-X100 or on 5-µm paraffin sections using antigen retrieval for 20 min in boiling, 10 mM citric acid, pH 6.0. For BrdU immunostaining, an additional incubation period of 10 min in 2N HCl was performed. For immunohistochemistry, endogenous peroxidases were blocked by incubation with 0.6% H₂O₂ in methanol. After incubation with the indicated antibodies, secondary fluorescently labelled antibodies Alexa Fluor 488, 567 and 647 (Molecular Probes, Invitrogen) or HRP-conjugated secondary antibodies were used to reveal the primary antibodies. For immunohistochemistry, Dako Envision⁺ was used together with diaminobenzidine tablets (Sigma) to detect HRP. Fluorescent images were made with an automated upright microscope system (DM5500, Leica) or an LSM700 upright or inverted confocal microscope (Zeiss). Light images were made with an AX70 widefield microscope (Olympus). Figures were generated with PHOTOSHOP (Adobe Systems) and CYTOSKETCH (CytoCode).

In situ hybridizations were performed on paraffin sections permeabilized by proteinase K digestion using DIG-labelled (Roche), antisense transcripts of the mouse **POSTN** complementary DNA. After hybridization, sections were washed in 50% formamide, ×5 SSC (0.75 M NaCl, 85 mM sodium citrate, pH 7.0) and 0.1% Tween at 70 °C, and non-specifically bound probe was digested by RNaseA treatment, followed by extensive washing in 50% formamide, ×2 SSC and 0.1% Tween at 65 °C. The DIG label was detected by an anti-DIG Fab (Roche) coupled to alkaline phosphatase using FAST NBT/BCIP (Sigma).

Western blot. Protein was extracted with complete RIPA buffer, separated by electrophoresis, transferred to PVDF membranes, blocked with 5% dry milk or BSA and incubated overnight with primary antibodies. Immunoreactive bands were visualized using HRP-conjugated secondary antibodies (Promega) and the detection reagent SuperSignal West Chemiluminiscent Substrate (Thermo Scientific).

Real-time RT-PCR. RNA was prepared using a miniRNA or microRNA kit (Qiagen) from FACS-isolated primary cells. Complementary DNAs were generated using oligo-T priming and quantitative PCR was performed in a LightCycler (Roche) or a StepOnePlus thermocycler (Applied Biosystems) using the Power SYBR green PCR Master Mix (Applied Biosystems) and the primers aatgctgcctggc tatat and gcatgaccctttctctca (POSTN); agccgacacacaacctag and ggggtctgccca catagtacaag (TGF-β3); and caagctcattctcgtatgacaat and gttggataggcctctctg (GAPDH).

Periostin monoclonal antibody production. In collaboration with Adipogen, we injected *Postn*^{-/-} mice with purified human POSTN protein. Hybridomas were generated and tested for antibody production by ELISA. Antibodies were selected for their ability to recognize POSTN and for their ability to block tumour mammosphere formation *in vitro*.

Periostin interactome and pull-downs. Freshly isolated tumour cells were grown under mammosphere conditions in the presence of purified, polyHis-tagged and streptavidin binding peptide (SBP)-tagged POSTN protein (Supplementary Fig. 28) for 72 h. Then proteins were crosslinked by 1 mM DTSSP (Pierce) for 10 min and solubilized by DDM and SDS (Anatrace). Protein purification was achieved by two successive affinity purification steps using the SBP and the polyHis tags and elution by biotin and imidazole, respectively. After elution, the crosslink was released by DTT treatment, the resulting protein mixture was trypsin-digested and peptides were identified by one-dimensional nano-liquid chromatography tandem mass spectrometry. Among the **POSTN**-attached proteins, we found Wnt6 to be a potential interactor. Because these experiments involved crosslinkers, we consider these results to be preliminary unless confirmed by independent experiments. For Wnt6, an interaction with **POSTN** could not be validated owing to a lack of Wnt6 antibodies and a suitable expression system for Wnt6. Nevertheless, this preliminary finding prompted us to test directly for interactions of **POSTN** with other Wnt ligands where the necessary tools are available. For these pull-downs, cDNAs encoding Wnt1, HA-tagged Wnt3A, DKK1 and SBP/His-tagged **POSTN** (Supplementary Fig. 28) or SBP/His-tagged mouse immunoglobulin-G heavy chain (as a control) were transfected separately into 293T cells. **Cells secreting POSTN or immunoglobulin-G and cells producing Wnt or DKK were mixed after one day and collected for pull-downs after three additional days.** Without the use of crosslinkers, POSTN-interacting proteins were enriched by the SBP/His tag as described above using NP40 as detergent. Western blot was performed for identification of the pulled-down proteins.

Wnt reporter activity. HEK293T cells were transduced with a lentiviral vector containing a LEF/TCF-responsive luciferase reporter consisting of a minimal promoter and 20 copies of the LEF/TCF consensus site or a control construct in which the LEF/TCF sites had been mutated³⁴. These stable Wnt reporter cell lines were then transiently transfected with a POSTN expression vector before these cells were mixed with transiently transfected HEK293T or COS7 cells (the latter for Wnt6 expression) producing Wnt1, Wnt2 or Wnt6, respectively. The media on these co-cultures of Wnt reporter and Wnt producer cells were replaced after 24 h to remove soluble Wnt ligands. After 48 h of co-culture, luciferase activity in cell extracts was measured with a kit from Promega.

For *in vivo* reporter assays, we generated a lentiviral vector containing the same transcription factor sites and minimal promoter as described above driving GFP expression. In addition, this vector contained a ubiquitous PGK promoter driving expression of a truncated human CD2 cDNA that allows identification of reporter-containing cells by FACS (Supplementary Fig. 29). Lentiviruses were generated in 293T cells using third-generation lentivirus packaging vectors, and virus particles were concentrated by ultracentrifugation. Freshly isolated tumour cells were infected with lentiviruses overnight, enriched by anti-CD2 MACS (Miltenyi) for cells carrying the reporter construct and orthotopically transplanted for tumour formation and spontaneous metastasis. Wnt signalling activity in cells of primary tumours or spontaneous pulmonary metastases was quantified by FACS analysis by measuring GFP⁺ cells after gating for human-CD2⁺ cells. Similarly, human-CD2⁺

tumour cells were used for tumour mammosphere cultures to measure Wnt pathway activity in the presence or absence of the POSTN blocking antibody.

Isolation of lung stromal cells. Lungs were minced with a razor blade and digested with a mixture of DNase and Liberase (Roche Diagnostics). On enzymatic digestion, samples were passed through a 100- μ m filter and washed once in growth medium (DMEM/F12 with 2% FBS, 20 ng ml⁻¹ EGF and 10 μ ml⁻¹ insulin; Invitrogen) and twice in PBS. Cells were plated onto plates pretreated with collagen and allowed to attach for three days. The medium was then changed to serum-free medium and tumour cells or soluble factors were added to test POSTN induction. POSTN expression was evaluated by western blot, PCR with reverse transcription or immunofluorescence analysis.

31. Guy, C. T., Cardiff, R. D. & Muller, W. J. Induction of mammary tumours by expression of polyomavirus middle T oncogene: a transgenic mouse model for metastatic disease. *Mol. Cell. Biol.* **12**, 954–961 (1992).
32. Tsukamoto, A. S., Grosschedl, R., Guzman, R. C., Parslow, T. & Varmus, H. E. Expression of the int-1 gene in transgenic mice is associated with mammary gland hyperplasia and adenocarcinomas in male and female mice. *Cell* **55**, 619–625 (1988).
33. Okabe, M., Ikawa, M., Kominami, K., Nakanishi, T. & Nishimune, Y. 'Green mice' as a source of ubiquitous green cells. *FEBS Lett.* **407**, 313–319 (1997).
34. Jeannot, G. *et al.* Long-term, multilineage hematopoiesis occurs in the combined absence of β -catenin and γ -catenin. *Blood* **111**, 142–149 (2008).